

Simultaneous synthesis and consolidation of nanostructured NbSi₂–Si₃N₄ composite from mechanically activated powders by high-frequency induction-heated combustion

Hyun-Kuk Park^a, In-Jin Shon^{a,*}, Jin-Kook Yoon^b, Jung-Mann Doh^b,
In-Yong Ko^a, Z.A. Munir^c

^a Department of Materials Engineering, Research Center of Advanced Material Development, Chonbuk National University, 664-14 Deokjin-dong 1-ga, Deokjin-gu, Jeonju, Jeonbuk 561-756, South Korea

^b Metal Processing Research Center, Korea Institute of Science and Technology, P.O. Box 131, Cheongryang, Seoul 136-791, South Korea

^c Facility for Advanced Combustion Synthesis, Department of Chemical Engineering and Materials Science, University of California, Davis, CA 95616, USA

Received 31 May 2007; received in revised form 2 July 2007; accepted 14 July 2007
Available online 25 July 2007

Abstract

Dense nanostructured 4NbSi₂–Si₃N₄ composite was synthesized by high-frequency induction-heated combustion synthesis (HFHCS) method within 1 min in one step from mechanically activated powders of NbN and Si. Simultaneous combustion synthesis and densification were accomplished under the combined effects of an induced current and mechanical pressure. Highly dense 4NbSi₂–Si₃N₄ composite with relative density of up to 98% was produced under simultaneous application of a 60 MPa pressure and the induced current. The average grain size and mechanical properties (hardness and fracture toughness) of the composite were investigated.

© 2007 Elsevier B.V. All rights reserved.

Keywords: High-frequency induction-heated combustion; Composite materials; Intermetallic; Sintering; Nanophase; Mechanical properties; NbSi₂–Si₃N₄

1. Introduction

Interest in refractory metal silicides has increased significantly in recent years because of their potential application as high-temperature structural materials [1]. This class of materials has an attractive combination of properties including high melting temperature, high modulus, high oxidation resistance in air, and a relatively low density [2,3]. However, as in the case of many intermetallic compounds, the current concern about these materials focuses on their low fracture toughness below the ductile–brittle transition temperature [4–6]. To improve on their mechanical properties, the approach commonly utilized has been the addition of a second phase to form composites [7–12]. An example is the addition of Si₃N₄ to NbSi₂ to improve the latter's properties. Silicon nitride has a high thermal shock resistance,

due to its low thermal expansion coefficient and a good resistance to oxidation when compared to other structural materials [13,14]. The isothermal oxidation resistance of NbSi₂–40 vol.% Si₃N₄ composite prepared by spark plasma sintering (SPS) process in dry air at 1300 °C was superior to that of monolithic NbSi₂ compact since the composite contained a larger amount of Si, which made it easier to form dense SiO₂ scale [15]. Therefore, Si₃N₄ may be the most promising additive as a reinforcing material for NbSi₂-based composites.

Many similar high-temperature dense composites are usually prepared in a multi-step process [16,17]. However, the method of field-activated and pressure-assisted combustion synthesis has been successfully employed to synthesize and densify materials from the elements in one step in a relatively shorter period of time. This method has been used to synthesize a variety of ceramics and composites, including MoSi₂–ZrO₂, Ti₅Si₃ and its composites, WSi₂ and its composites, and WC–Co hard materials [18–23]. These materials, which are generally characterized by low adiabatic combustion temperature, cannot be

* Corresponding author. Tel.: +82 63 270 2381; fax: +82 63 270 2386.
E-mail address: ijshon@chonbuk.ac.kr (I.-J. Shon).

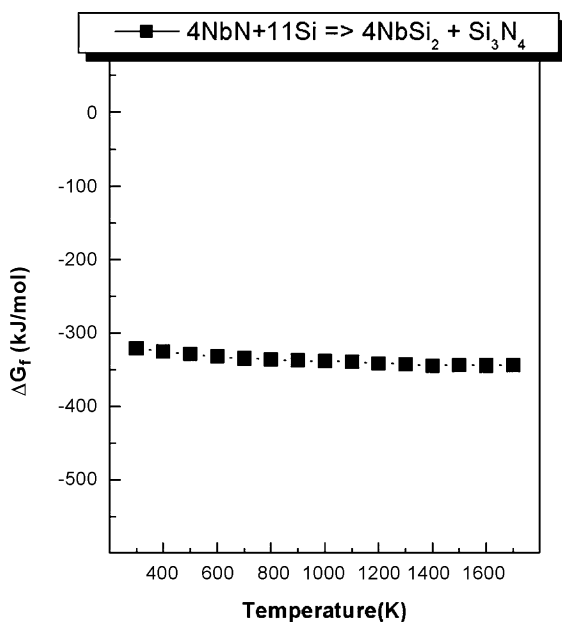
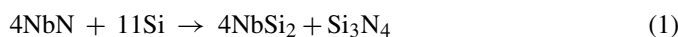


Fig. 1. Temperature dependence of the Gibbs free energy for the interaction between NbN and silicon.

synthesized directly by the self-propagating high-temperature synthesis (SHS) method. More recently, a new approach has been developed in which synthesis and densification can be affected simultaneously. This new process, referred to as the high-frequency induction-heated combustion synthesis (HFHCS), has been successfully used to synthesize and densify materials in one step in a relatively shorter period of time (2 min) [24–26].

The objective of this study is to investigate the preparation of dense nanophase $4\text{NbSi}_2\text{--Si}_3\text{N}_4$ composite by the HFHCS method starting from a mixture of mechanically activated NbN and Si powders. The interaction between these phases, i.e.,



is thermodynamically feasible, as can be seen from Fig. 1.

2. Experimental procedure

Powders of 99.97% pure niobium nitride (–325 mesh, Alfa Products, Ward Hill, MA) and 99.5% pure silicon (–325 mesh, Alfa Products, Ward Hill, MA) were used as starting materials. Fig. 2 shows the SEM images of the raw materials used. Powder mixtures of NbN and Si in the molar proportion of 4:11 were first milled in a high-energy ball mill (Pulverisette-5, planetary mill) at 250 rpm for 10 h. Tungsten carbide balls (5 mm in diameter) were used in a sealed cylindrical stainless steel vial under argon atmosphere. The weight ratio of ball-to-powder was 30:1. Milling resulted in a significant reduction of grain size. The grain size and the internal strain were calculated by Stokes and Wilson's formula [27]:

$$b = b_d + b_e = \frac{k\lambda}{d \cos \theta + 4\varepsilon \tan \theta}$$

where b is the full width at half-maximum (FWHM) of the diffraction peak after instrument correction, b_d and b_e are FWHM caused by small grain size and internal stress, respectively, k the constant (with a value of 0.9), λ the wavelength of the X-ray radiation, d and ε are grain size and internal stress, respectively, and θ is the Bragg angle. The parameters b and b_s follow Cauchy's form with the relationship: $B_0 = b + b_s$, where B_0 and b_s are FWHM of the broadened Bragg peaks and the standard sample's Bragg peaks, respectively. Fig. 3 shows the XRD patterns of the raw powders and the milled $4\text{NbN} + 11\text{Si}$ powder mixture.

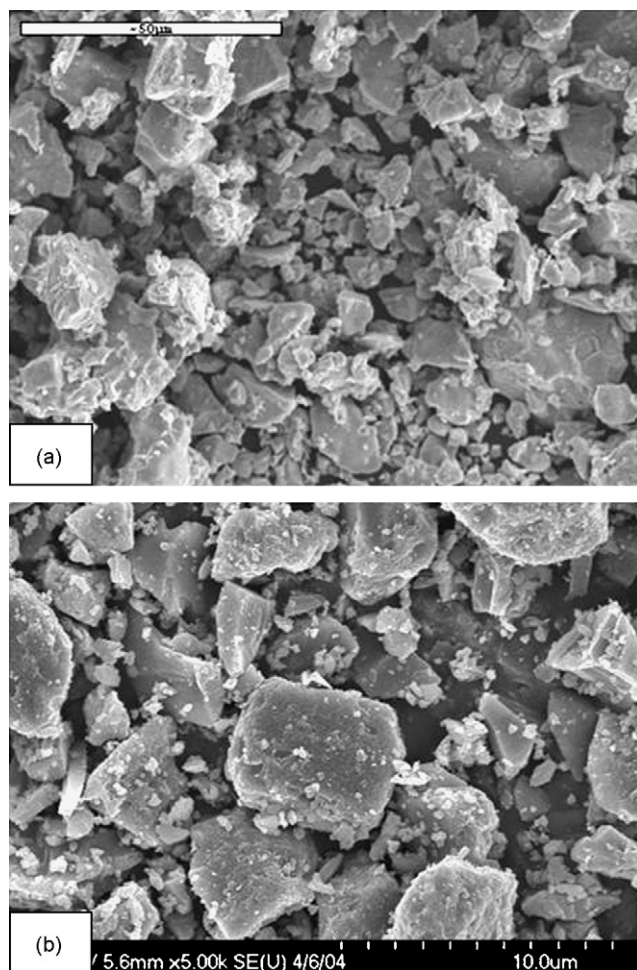


Fig. 2. Scanning electron microscope images of raw materials: (a) niobium nitride and (b) silicon.

The FWHM of the milled powder is greater than that of the raw powders due to internal strain and grain size reduction. The average grain sizes of the milled NbN and Si powders were determined as 75 and 22 nm, respectively.

After milling, the mixed powders were placed in a graphite die (outside diameter, 45 mm; inside diameter, 20 mm; height, 40 mm) and then introduced into the high-frequency induction-heated combustion system [28]. Following the introduction of the die into the apparatus, the system was evacuated and a uniaxial pressure of 60 MPa was applied. An induced current (frequency of about 50 kHz) was then activated and maintained until densification was attained as indicated by a linear gauge measuring the shrinkage of the sample. Temperatures were measured by a pyrometer focused on the surface of the graphite die. At the end of the process, the sample was cooled to room temperature. The process was carried out under a vacuum of 40 mTorr.

The relative densities of the synthesized sample were measured by the Archimedes method. Microstructural characterization was made on product samples which had been polished and etched using a solution of HF (10 vol.%), HNO_3 (30 vol.%), and H_2O (60 vol.%) for 1 min at room temperature. Compositional and microstructural analyses of the products were made through X-ray diffraction (XRD) and scanning electron microscopy (SEM) with energy dispersive X-ray analysis (EDAX). Vickers hardness was measured by performing indentations at a load of 10 kg and a dwell time of 15 s.

3. Results and discussion

The variations in shrinkage displacement and temperature with heating time during the processing of $4\text{NbN} + 11\text{Si}$ system

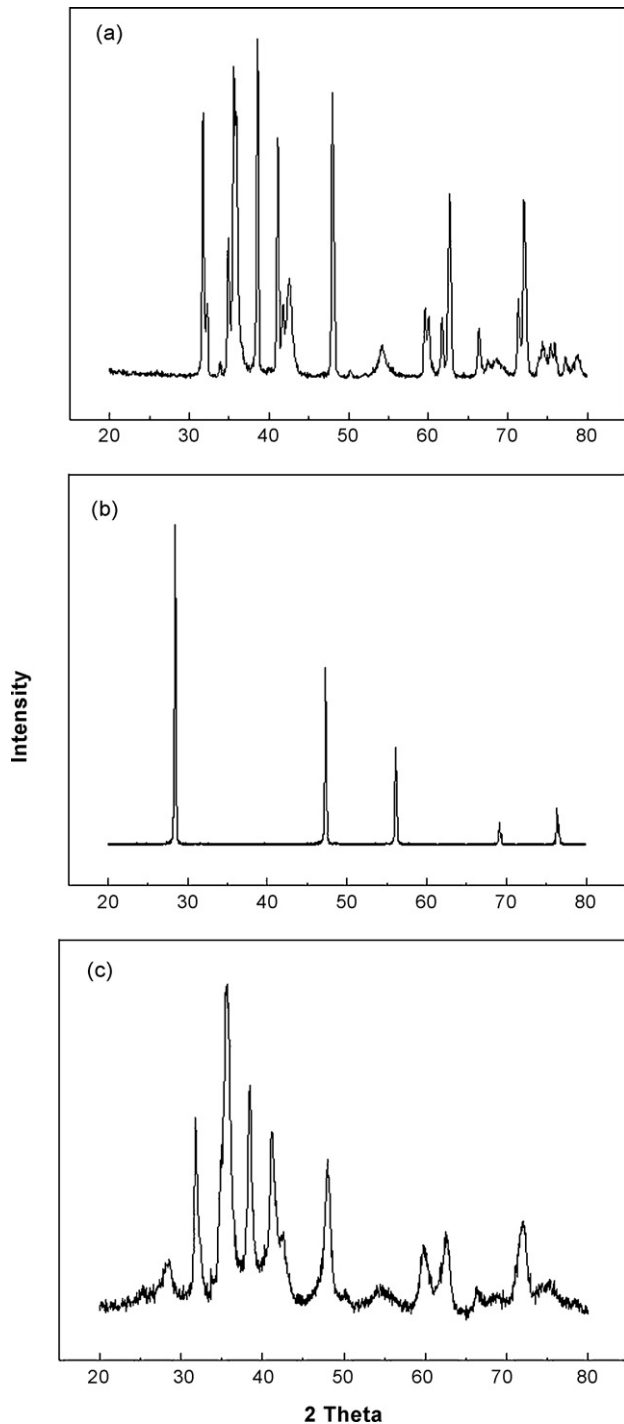


Fig. 3. XRD patterns of raw materials: (a) NbN, (b) Si, and (c) milled $4\text{NbN} + 11\text{Si}$.

are shown in Fig. 4. As the induced current was applied, the reactant powders (Fig. 4(a)) shows initially a small (thermal) expansion and the shrinkage displacement increased gradually with temperature up to 800°C (Fig. 4(b)), but then abruptly increased at about 850°C . When the reactant mixture of $4\text{NbN} + 11\text{Si}$ was heated under 60 MPa pressure to 800°C , no reaction took place and no significant shrinkage displacement as judged by subsequent XRD and SEM analyses. Fig. 5(a–c) shows the SEM (secondary electron) images of (a) powder after

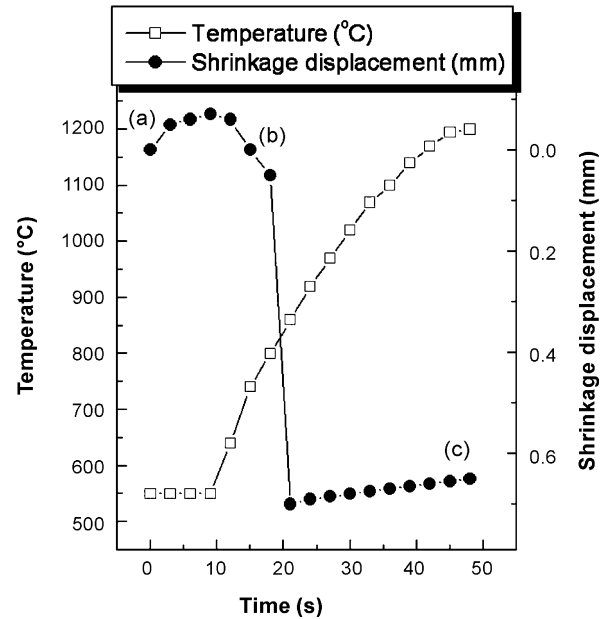


Fig. 4. Variations of temperature and shrinkage displacement with heating time during high-frequency induction-heated combustion synthesis and densification of $4\text{NbSi}_2\text{-Si}_3\text{N}_4$ composite (under 60 MPa and 90% output of total power capacity).

milling, (b) sample heated to 800°C , and (c) sample heated to 1200°C , respectively. Fig. 5(a and b) shows the presence of the reactants as separate phases. X-ray diffraction results, shown in Fig. 6(a and b) exhibit only peaks pertaining to the reactants NbN and Si. However, when the temperature was raised to 1200°C , the starting powders reacted producing highly dense products (Fig. 4(c)). SEM image of an etched surface of the samples heated to 1200°C under a pressure of 60 MPa is shown in Fig. 5(c). A complete reaction between NbN and Si took place under these conditions. X-ray diffraction analyses of this sample showed peaks of only NbSi_2 and Si_3N_4 , as indicated in Fig. 6(c). The abrupt increase in the shrinkage displacement at the ignition temperature is due to the increase in density as a result of molar volume change associated with the formation of $4\text{NbSi}_2\text{-Si}_3\text{N}_4$ from the reactants (NbN and Si) and the consolidation of the product. It should be recalled that the measured temperatures are those of the surface of the die and are, therefore, likely to be different than the values in the middle of the sample. Thus, the onset of the reaction to form the composite (and the concomitant rapid shrinkage) may be at a higher temperature than the observed value of 850°C . As the imposition of an induced electric field increases the combustion temperature for 4NbN and 11Si system, it is expected that Si would be molten during the continuation of the reaction. Once the liquid is formed, its further formation and spreading over the NbN particles are fast, due to surface energy. As soon as the liquid penetrates the particles boundaries, a tremendous capillary force is developed which leads to particle rearrangement and pore filling for closer packing in the presence of Si liquid phase [29]. In this stage, NbN continuously reacts with Si into NbSi_2 and Si_3N_4 . And then grain growth and densification occur simultaneously under high pressure. This is most likely the reason for the significant

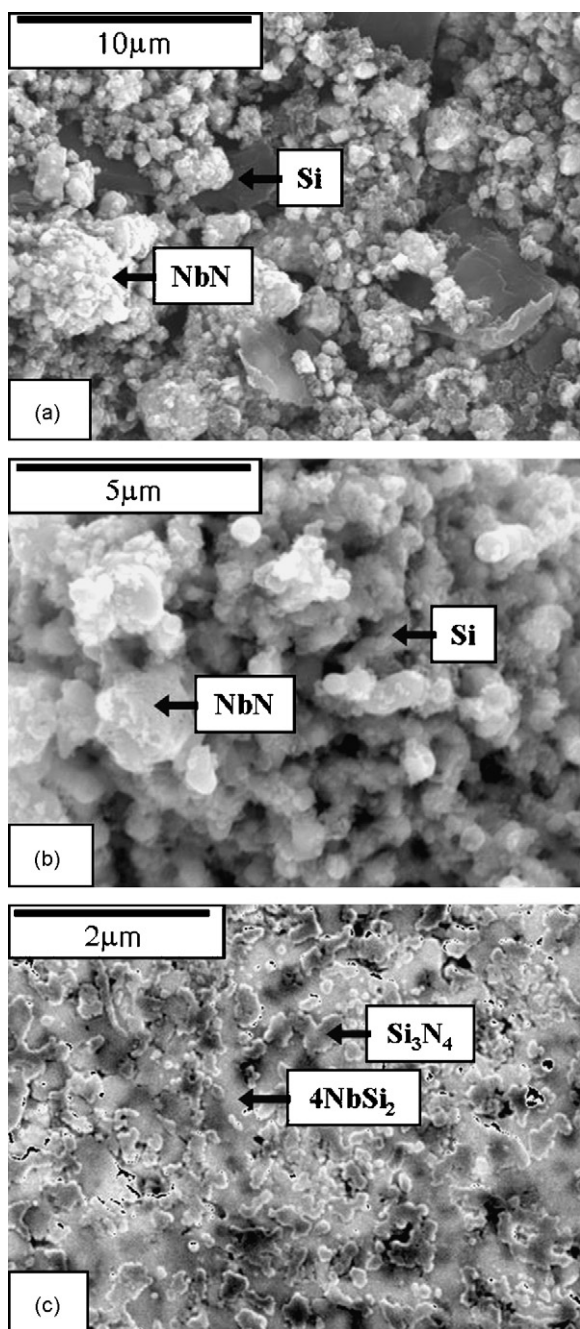


Fig. 5. Scanning electron microscope images of 4NbN + 11Si system: (a) after milling, (b) before combustion synthesis, and (c) after combustion synthesis.

increase in shrinkage beyond the value dictated by the molar volume change. The relative density of the product is about 98%. This result is thought to be due to the formation of the liquid phase during combustion synthesis, which can easily reduce the porosity under mechanical pressure.

The average grain sizes of NbSi₂ and Si₃N₄ calculated by the Stokes–Wilson formula [27] were about 90 and 25 nm. The Si₃N₄ particles were well distributed in matrix, as can be seen from the SEM image, Fig. 5(c).

Vickers hardness measurements were made on polished sections of the NbSi₂–Si₃N₄ composite using a 10 kg load and 15 s dwell time. The calculated hardness value, based on an aver-

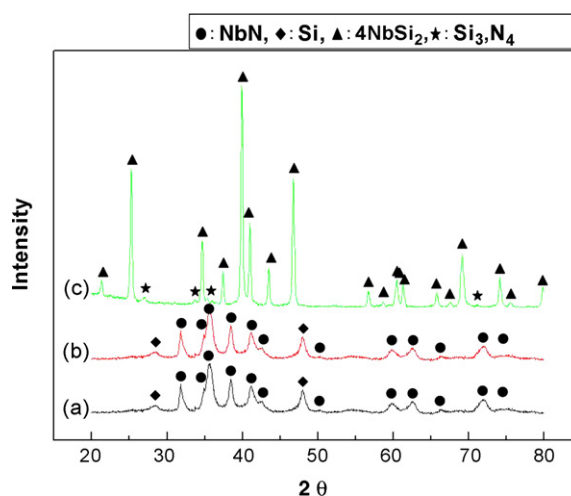


Fig. 6. XRD patterns of the 4NbN + 11Si system: (a) after milling, (b) before combustion synthesis, and (c) after combustion synthesis.

age of five measurements, of the NbSi₂–Si₃N₄ composite is 680 kg mm⁻². Indentations with large enough loads produced median cracks around the indent. The length of these cracks permits an estimation of the fracture toughness of the materials by means of the expression [30]:

$$K_{IC} = 0.204 \left(\frac{c}{a} \right)^{-3/2} H_v a^{1/2}$$

where c is the trace length of the crack measured from the center of the indentation, a the half of average length of two indent diagonals, and H_v is the hardness. A typical indentation pattern for the 4NbSi₂–Si₃N₄ composite is shown in Fig. 7(a). Typically, one to three additional cracks were observed to propagate from the indentation corner. The calculated fracture toughness value for the NbSi₂–Si₃N₄ composite is about 3.1 MPa m^{1/2}. As in the case of the hardness value, the toughness value is the average of measurements on five measurements. Higher magnification view of the indentation median crack in the composite is shown in Fig. 7(b). This shows the crack propagates along phase boundary of NbSi₂ and Si₃N₄.

The absence of reported values for hardness and toughness on NbSi₂–Si₃N₄ precludes making direct comparison to the results obtained in this work to show the influence of grain size. Similarly, an absence of corresponding data on NbSi₂ makes it difficult to show the effect of the addition of Si₃N₄. The only related study reported in the literature is that we are cognizant by Guille and Matini [31]. They investigated the microhardness and fracture toughness of silicide coatings on metal substrates. Coatings of thicknesses ranging from 30 to 40 μm were formed. In the case of Nb substrates, the coating was composed of a layer NbSi₂ only. It was found that the hardness of NbSi₂ depended on the applied load, being constant, at a value of about 10 GPa, in the load range of 0.15–0.6 N, but increased linearly at higher loads. The calculated fracture toughness, however, was independent of load, being about 2 MPa m^{1/2}. Although a direct comparison cannot be made, but the hardness of our composite is significantly lower than the lowest value of about 10 GPa at 0.15–0.6 N in the reported literature account results. Likewise, the frac-

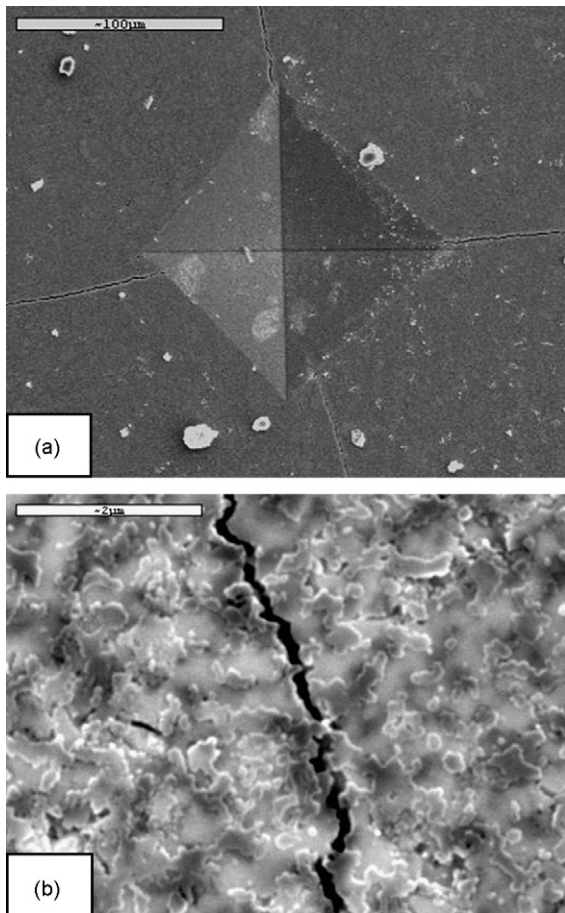


Fig. 7. (a) Vickers hardness indentation and (b) median crack propagating of $4\text{NbSi}_2\text{-Si}_3\text{N}_4$ composite.

ture toughness in the composite of this work ($3.1 \text{ MPa m}^{1/2}$) is more than 50% higher than the value in the cited reference [31].

4. Summary

Using the high-frequency induction-heated combustion method, the simultaneous synthesis and densification of nanostructured $4\text{NbSi}_2\text{-SiC}$ composite was accomplished using powders of NbN and Si . Complete synthesis and densification can be achieved in one step within 1 min. The relative density of the composite was 98% under an applied pressure of 60 MPa and the induced current. The average grain sizes of NbSi_2 and Si_3N_4 phases in the composite were about 90 and 25 nm, respectively. The average hardness and fracture toughness values obtained were 680 kg mm^{-2} and $3.1 \text{ MPa m}^{1/2}$, respectively. The lack of reported data on $\text{NbSi}_2\text{-Si}_3\text{N}_4$ makes difficult to make direct comparisons, but based on reported data on NbSi_2 coating, an

approximate comparison shows that the present results exhibit a lower hardness and higher toughness.

Acknowledgments

We are grateful for the financial support from the Korea Institute of Science and Technology, which was provided through the program for study on Technologies for Formation and Evaluation of Nanostructured Composite Coatings. The support of the US Army Research Office (ARO) to one of us (ZAM) is acknowledged.

References

- [1] N.S. Stoloff, *J. Mater. Sci. Eng. A* 261 (1999) 169–180.
- [2] A.K. Vasudevan, J.J. Petrovic, *J. Mater. Sci. Eng. A* 155 (1992) 259–266.
- [3] G.J. Fan, M.X. Quan, Z.Q. Hu, J. Eckert, L. Schulz, *Scripta Mater.* 41 (1999) 1147–1151.
- [4] G. Sauthoff, *Intermetallics*, VCH Publishers, New York, 1995.
- [5] Y. Ohya, M.J. Hoffmann, G. Petzow, *J. Mater. Sci. Lett.* 12 (1993) 149–152.
- [6] J. Qian, L.L. Daemen, Y. Zhao, *Diamond Relat. Mater.* 14 (2005) 1669–1672.
- [7] B.W. Lin, T. Iseki, *Br. Ceram. Trans. J.* 91 (1992) 1–5.
- [8] Y. Ohya, M.J. Hoffmann, G. Petzow, *J. Am. Ceram. Soc.* 75 (1992) 2479–2483.
- [9] S.K. Bhaumik, C. Divakar, A.K. Singh, G.S. Upadhyaya, *J. Mater. Sci. Eng. A* 279 (2000) 275–281.
- [10] D.K. Jang, R. Abbaschian, *Korean J. Mater. Res.* 9 (1999) 92–98.
- [11] H. Zhang, P. Chen, M. Wang, X. Liu, *Rare Met.* 21 (2002) 304–307.
- [12] D.Y. Oh, H.C. Kim, J.K. Yoon, I.J. Shon, *J. Alloys Compd.* 395 (2005) 174–180.
- [13] W. Dressler, R. Riedel, *Int. J. Refract. Met. Hard Mater.* 15 (1997) 13–47.
- [14] S.P. Taguchi, S. Ribeiro, *J. Mater. Process. Technol.* 147 (2004) 336–342.
- [15] T. Murakami, S. Sasaki, K. Ichikawa, A. Kitahara, *Intermetallics* 9 (2001) 621–628.
- [16] K. Bhattacharya, J.J. Petrovic, *J. Am. Ceram. Soc.* 74 (1991) 2700–2703.
- [17] Y. Luo, S. Li, W. Pan, L. Li, *Mater. Lett.* 58 (2003) 150–153.
- [18] Z.A. Munir, I.J. Shon, K. Yamazaki, US Patent 5,794,113 (1998).
- [19] I.J. Shon, Z.A. Munir, K. Yamazaki, K. Shoda, *J. Am. Ceram. Soc.* 79 (1996) 1875–1880.
- [20] I.J. Shon, H.C. Kim, D.H. Rho, Z.A. Munir, *Mater. Sci. Eng. A* 269 (1999) 129–135.
- [21] I.J. Shon, D.H. Rho, H.C. Kim, Z.A. Munir, *J. Alloys Compd.* 322 (2001) 120–126.
- [22] I.J. Shon, D.H. Rho, H.C. Kim, *Met. Mater.* 6 (2000) 533–541.
- [23] C.D. Park, H.C. Kim, I.J. Shon, Z.A. Munir, *J. Am. Ceram. Soc.* 85 (2002) 2670–2677.
- [24] H.C. Kim, D.Y. Oh, I.J. Shon, *Int. J. Refract. Met. Hard Mater.* 22 (2004) 41–49.
- [25] H.C. Kim, D.Y. Oh, J. Guojian, I.J. Shon, *Mater. Sci. Eng. A* 368 (2004) 10–17.
- [26] D.Y. Oh, H.C. Kim, J.K. Yoon, I.J. Shon, *J. Alloys Compd.* 395 (2005) 270–275.
- [27] F.L. Zhang, C.Y. Wang, M. Zhu, *Scripta Mater.* 49 (2003) 1123–1128.
- [28] H.C. Kim, D.Y. Oh, I.J. Shon, *Ref. Met. Hard Mater.* 22 (2004) 41–49.
- [29] S.L. Kharatyan, H.A. Chatilyan, *Int. J. SHS* 8 (1999) 31–38.
- [30] N. Koichi, *Ceramics* 20 (1985) 1218–1224.
- [31] J. Guille, L. Matini, *J. Mater. Sci. Lett.* 7 (1988) 952–954.